Stability of Materials

Edited by

A. Gonis and
P. E. A. Turchi

Lawrence Livermore National Laboratory
Livermore, California

and

Josef Kudrnovský

Czech Academy of Sciences
Praha, Czech Republic

Plenum Press
New York and London
Published in cooperation with NATO Scientific Affairs Division

Proceedings of a NATO Advanced Study Institute on
Stability of Materials,
held June 25 – July 7, 1994,
in Corfu, Greece

NATO-PCO-DATA BASE

The electronic index to the NATO ASI Series provides full bibliographical references (with keywords and/or abstracts) to about 50,000 contributions from international scientists published in all sections of the NATO ASI Series. Access to the NATO-PCO-DATA BASE is possible in two ways:

—via online FILE 128 (NATO-PCO-DATA BASE) hosted by ESRIN, Via Galileo Galilei, I-00044 Frascati, Italy

—via CD-ROM "NATO Science and Technology Disk" with user-friendly retrieval software in English, French, and German (©WTV GmbH and DATAWARE Technologies, Inc. 1989). The CD-ROM contains the AGARD Aerospace Database.

The CD-ROM can be ordered through any member of the Board of Publishers or through NATO-PCO, Overijse, Belgium.

Library of Congress Cataloging-in-Publication Data

Stability of materials / edited by A. Gonis, P.E.A. Turchi, and Josef Kudrnovský.
p. cm. -- (NATO ASI series. Series B, Physics ; v. 355)
"Published in cooperation with NATO Scientific Affairs Division."
"Proceedings of a NATO Advanced Study Institute on Stability of Materials, held June 25-July 7, 1994, in Corfu, Greece"--T.p. verso.
Includes bibliographical references and index.
ISBN 0-306-45311-8
1. Electronic structure--Congresses. 2. Alloys--Mathematical models--Congresses. 3. Materials--Mathematical models--Congresses. I. Gonis, Antonios, 1945- . II. Turchi, Patrice E. A. III. Kudrnovský, Josef. IV. North Atlantic Treaty Organization. Scientific Affairs Division. V. NATO Advanced Study Institute on Stability of Materials (1994 : Kerkyra, Greece) VI. Series.
QC176.8.E35S73 1996
620.1'1299--dc20 96-18486
CIP

ISBN 0-306-45311-8

A Division of Plenum Publishing Corporation
233 Spring Street, New York, N. Y. 10013

10 9 8 7 6 5 4 3 2 1

Printed in the United States of America

CRYSTAL STRUCTURE AND PHYSICAL PROPERTIES OF HIGH PRESSURE HYDRIDES

V.E. Antonov

Institute of Solid State Physics
Russian Academy of Sciences
142432 Chernogolovka Moscow distr.
Russia

INTRODUCTION

The technique for compressing gaseous hydrogen to pressures of up to 9 GPa at temperatures to 500 °C (and recently[1] to 1000 °C) developed at ISSP RAS made it possible to synthesize bulk homogeneous hydrides of a number of Group VI–VIII transition metals which cannot be hydrogenated by standard procedures[2]. This enabled us to prepare hydrides of all $3d$- and $4d$-metals (except ruthenium) and of many their alloys, and to systematically study their crystal structure and physical properties as function of the position of the initial metals in the Periodic Table (Fig. 1). Most of the hydrides are nonstoichiometric interstitial phases (solid hydrogen solutions) with wide homogeneity ranges of composition, that allowed the investigation of their properties as function of the hydrogen concentration as well.

In order to explain the observed dependences of the magnetic properties of the $3d$-metals and their alloys on the hydrogen content, the phenomenological rigid d-band model was proposed[2,3]. Studies of the superconducting properties of high pressure hydrides of the $4d$- and $5d$-metals and their alloys led to the discovery of new superconducting hydrides[4–6] and showed that with proper corrections for the hydrogen-induced changes in the phonon spectra, the rigid d-band model could also be used to explain the observed superconducting phenomena[5]. And finally, the model was found to be applicable to the description of the crystal structures of the hydrides for rather large groups of d-metals and alloys[6].

The model seems to be the only guide now allowing understanding and, under certain conditions, predicting the magnetic and superconducting properties and crystal structures of the transition metal hydrides, and below we shall briefly discuss how it works.

Stability of Materials
Edited by A. Gonis *et al.*, Plenum Press, New York, 1996

$\alpha \rightarrow \varepsilon$	$\alpha' \rightarrow \varepsilon,\gamma$	$\alpha \rightarrow \varepsilon'$	$\varepsilon \rightarrow \varepsilon,\gamma$	$\gamma \rightarrow \gamma$	γ
$CrH_{1.0}$	$MnH_{0.96}$	$FeH_{0.8}$	$CoH_{1.0}$	$NiH_{1.1}$	Cu
af → p	af → af	f → f	f → f	f → p	d
$\alpha \rightarrow \varepsilon$	$\varepsilon \rightarrow \varepsilon$	$\varepsilon \rightarrow \varepsilon$	$\gamma \rightarrow \gamma$	$\gamma \rightarrow \gamma$	γ
$MoH_{1.05}$	$TcH_{0.6}$	$RuH_{0.03}$	$RhH_{1.0}$	$PdH_{1.0}$	Ag
sc → sc	sc → sc	sc → sc	p → p	p → sc	d
α	$\varepsilon \rightarrow \varepsilon$	$\varepsilon \rightarrow \varepsilon$	γ	γ	γ → orth
W	$ReH_{0.22}$	$OsH_{0.003}$	Ir	Pt	$AuH_{0.4}$
sc	sc → sc	sc → sc	sc	p	d

Figure 1. Hydrides synthesized under high hydrogen pressures[2]. The indicated hydrogen concentrations are the maximum attained ones. The arrows show the direction of the changes in the crystal structure and magnetic and superconducting properties of the starting metals on hydrogenation. Metal lattices: α = *bcc*, α' = α-Mn type, ε = *hcp*, ε' = *dhcp*, γ = *fcc*, orth = orthorombic. Magnetic state at low temperatures: af = antiferromagnetic, f = ferromagnetic, p = paramagnetic, d = diamagnetic. sc = superconductor. The hydrides of Fe, Co, Mo, Tc, Rh, Re, and Au were first synthesized at ISSP RAS.

MAGNETIC PROPERTIES

The rigid *d*-band model takes into account the specific changes in the band structure of transition metals on hydrogen uptake first outlined by A.C. Switendick[7] and then confirmed by many other calculations for various *d*-metals. According to the calculations, the hydrogen leaves the upper part of the *d*-band of the host metal nearly unaffected, but noticeably decreases the energy of the *s*-states. The latter lowers the rate, η, of *d*-band filling with the electrons supplied by the hydrogen to a value of the order of $\eta = 0.5$ electrons per H atom (varying from ≈ 0.3 to ≈ 1 for different metals and alloys). This concept implies that those properties of the metal which essentially depend on the *d*-band occupation should vary with increasing hydrogen concentration as if the hydrogen were merely donor of a fractional number of $\eta \approx 0.5$ electrons per atom into the otherwise unchanged metal *d*-band. This is the approximation that we call a rigid *d*-band model for brevity.

The 3*d*-metals, which are close neighbors in the Periodic Table, form broad ranges of *fcc* (γ) and *hcp* (ε) continuous solid solutions with magnetic properties well described by the rigid band model[8]. These properties thus can be represented by unique functions of the average number N^e of external $(3d + 4s)$ electrons per atom of the alloy (the so-called Pauling–Slater curves), see Fig. 2. The properties of the γ and ε hydrides of such alloys should therefore be the same functions of the effective electron concentration $N^e_{\text{eff}} = N^e + \eta \cdot n$, where n is the H–to–metal atomic ratio.

The available data on the hexagonal hydrides are presented in Fig. 2 and agree with this statement. As for the cubic hydrides, such an agreement can be most clearly demonstrated in the case of the Fe-Ni-H γ-solutions, see Fig. 3.

The spontaneous magnetization σ_0 at $T = 0$ K of the alloys containing up to 60 at.% Fe decreases approximately linearly with increasing n (Fig. 3*a*) and increasing

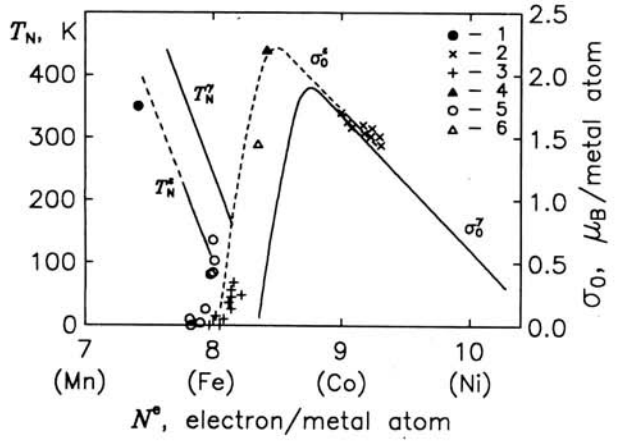

Figure 2. Concentration dependences[3] of σ_0 and Néel temperature, T_N, for the *fcc* (γ) (solid lines, experimental data) and *hcp* (ε) (sections of solid lines, experimental data, and dashed lines, an estimation) alloys of 3*d*-metals that are nearest neighbors in the Periodic Table, and also the experimental values of T_N for the antiferromagnetic manganese ε-hydride (1) and of σ_0 for the ferromagnetic ε-solutions Co-H (2), $Fe_{77.6}Mn_{22.4}$-H (3), ε'-hydride of iron (4), ε-hydrides $Fe_{75}Cr_{25}$-H (5), and $Fe_{94.7}Cr_{5.3}$-H hydride with a Sm-type metal lattice (6) at $\eta = 0.5$ el. per H atom.

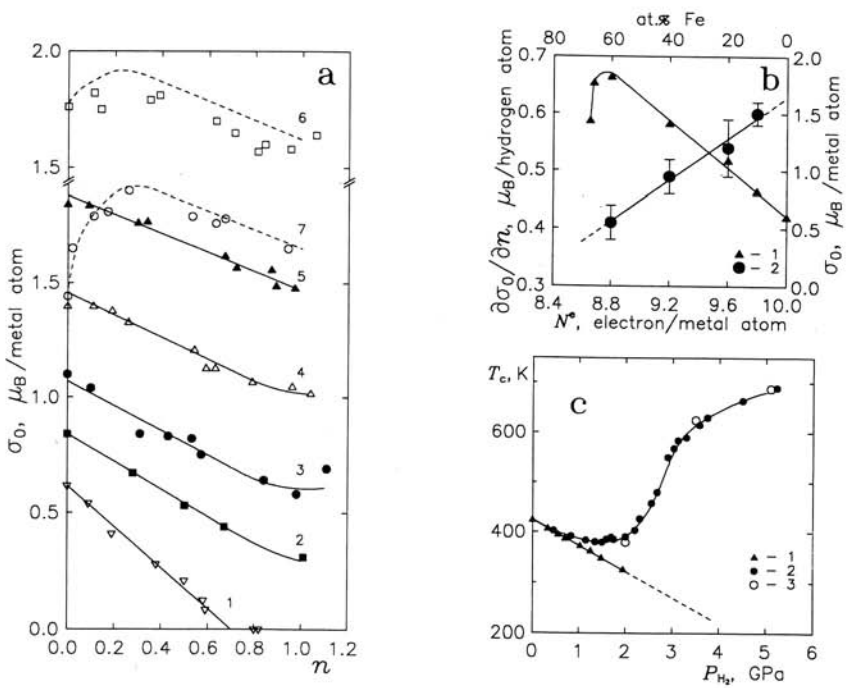

Figure 3. The effect of hydrogen on the magnetic properties of *fcc* Ni-Fe alloys[2]. (a) The spontaneous magnetization σ_0 at $T = 0$ K and under ambient pressure as function of the hydrogen–to–metal atomic ratio n. At. % Fe: 1 – 0, 2 – 10, 3 – 20, 4 – 40, 5 – 60, 6 – 66.1, 7 – 67.5. μ_B is Bohr magneton. (b) The spontaneous magnetization σ_0 of the Ni-Fe alloys (1) and the slope of the approximately linear dependences $\sigma_0(n)$ for the solid hydrogen solutions in the alloys containing 10, 20, 40, and 60 at. % Fe (2) as functions of the average number N^e of $(3d + 4s)$ electrons per atom in the initial *fcc* Ni-Fe alloys. (c) The experimental pressure dependences of the Curie temperatures T_c of the $Ni_{32.5}Fe_{67.5}$ alloy in an inert medium (1) and in hydrogen (2), and the $T_c(P_{H_2})$ values (3) calculated for $\eta = 0.39$ el. per H atom.

N^e (Fig. 3*b*, $\partial\sigma_0/\partial N^e \approx 1$ el./metal atom). The linear extrapolation of the coefficient of proportionality $\eta = (\partial\sigma_0/\partial n)/(\partial\sigma_0/\partial N^e)$ gives $\eta \approx 0.39$ el./hydrogen atom for the alloys with 66.1 and 67.5 at.% Fe (Fig. 3*b*). The $\sigma_0(n)$ dependences for these alloys (dashed lines in Fig. 3*a*) constructed from the $\sigma_0(N^e)$ dependence (Fig. 3*b*) using this scaling factor η, agree with the experiment. A good agreement is also observed between the experimental $T_c(P_{H_2})$ dependence for the $Ni_{32.5}Fe_{67.5}$ alloy (Fig. 3*c*) and the values calculated from the $T_c(N^e)$ and $dT_c(N^e)/dP$ dependences for the alloys without hydrogen using the same factor $\eta = 0.39$ el./hydrogen atom (the hydrogen concentration of the alloy in a hydrogen atmosphere monotonously increases on going along the $T_c(P_{H_2})$ line up to $n \approx 1$ at $P_{H_2} = 5.1$ GPa).

Magnetic properties were also studied for the hydrogen γ solutions in many other alloys of 3*d*-metals, including the alloys in which changes in the composition resulted in a strong deformation of the *d*-band (Ni-Cr, Ni-Mn). In all cases the rigid *d*-band model provided at least semiquantitative descriptions of the observed effects[2].

SUPERCONDUCTIVITY

In contrast to alloys of 3*d*-metals, the applicability of the rigid band model to alloys of 4*d*- and 5*d*-metals is usually limited to intervals of a few atomic per cent. There is a correlation, however, known as Matthias rule, between the superconducting temperature T_c and the electron concentration N^e, and the available data make it possible to specify at least one more type of alloys (let us call it *RN*, "remote plus neighboring") with superconducting properties obeying the rigid band model. These are $A_{1-y}(B,C,\ldots)_y$ alloys or intermetallic compounds with fixed y, where the elements B, C, *etc.*, are close neighbors, whereas element A is positioned far from them in the Periodic Table. In such systems replacing, for instance, element B by element C or varying their relative concentrations produces only minor changes in the band structure of the alloy. Wherever data are available, the Matthias plots for these *RN* type alloys and primary solid solutions of neighboring elements exhibit a large broad peak of T_c centered at $N^e \approx 6.3$ to 6.7 el./metal atom.

The formula $T_c(n) = T_c(N^e + \eta \cdot n) \approx T_c(N^e + 0.5 \cdot n)$ semiquantitatively describes the experimental $T_c(n)$ dependences for hydrogen solid solutions in *hcp* Re, Ru and Tc and accounts for the absence of superconductivity in the *fcc* Rh hydride with $N^e_{eff} \approx 9.5$ el./atom and for its presence in the *hcp* Mo hydride and the *fct* dihydride of the $Nb_{88}Rh_{12}$ alloy with $N^e_{eff} \approx 6.5$ el./atom (see ref. 6 for references). As one can see from Fig. 4, this formula is also more or less acceptable in the case of the hydrides with the *A*15 metal lattice.

In the hydrides on the base of *bcc* and related metal lattices, such as the *A*15 lattice, the *d*-band filling is not, however, an unconditionally dominating mechanism[5]. The changes caused by the *d*-band occupation are accompanied with a steady decrease in T_c at a rate τ of the order of -5 to -10 K per hydrogen atom. This is presumably due to a hardening of the acoustic phonon modes of the host metal (note, that the dissolved hydrogen causes an increase in the mean frequency of acoustic vibrations in *bcc* Nb and Ta metals[10], but a decrease in *fcc* Pd and Ni hydrides and *hcp* Mn hydride[11]). With both contributions taken together, the $T_c(n)$ dependence for the *bcc* and related alloys may be written as

$$T_c(n) \approx T_c(N^e + 0.5 \cdot n) - \tau \cdot n. \qquad (1)$$

This formula describes the $T_c(n)$ dependences for hydrogen solutions in the

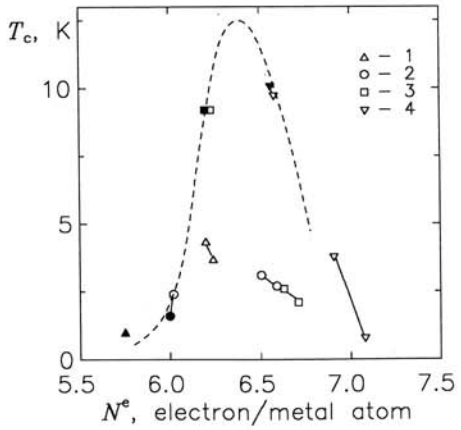

Figure 4. The superconducting temperature, T_c, as function of the electron concentration N^e for the initial samples Nb_3Me (blackened symbols) and as function of effective electron concentration $N^e + \eta \cdot n$ at $\eta = 0.5$ el./hydrogen atom for the Nb_3Me-H solid solutions[5]. Me = Os (1), Ir (2), Pt (3), and Au (4). The dashed line shows the $T_c(N^e)$ dependence for the $A15$ compounds of niobium and molybdenum with $5d$-metals[9].

Nb_3Me alloys (Fig. 4), *bcc* Nb-Ti alloys, and in the $Nb_{65}Rh_{35}$ alloy with a $D8_b$ type metal lattice (another *bcc*–related structure)[5,6].

CRYSTAL STRUCTURES

There are more and more indications (see, *e.g.*, refs. 12,13 and references therein) that the crystal structures of transition metals and alloys, with the possible exception of magnetic Mn, Fe, Co and Ni, are to a large extent determined by the d-band occupation and, as a consequence, by the electron concentration N^e. In particular, because of a strong dependence of the superconducting properties of the metals upon their crystal structure, the existence of the Matthias rule implies by itself such a correlation.

With correlations of this kind existing in pure metals as well as their alloys and intermetallic compounds, one should also expect similar correlations between the crystal structures and N^e_{eff} of the hydrides of transition metals and their alloys.

Phase transformations observed in the metal-hydrogen systems at high pressures are illustrated by Fig. 5. Where available, the lines of decomposition of the phases with higher hydrogen content are plotted, because these should be closer to the lines of the phase equilibria than the lines of formation of such phases (an analysis of the hysteresis phenomena in metal-hydrogen systems is given, *e.g.*, in refs. 14,15).

The equilibrium composition of the phases varies with the pressure and temperature within the single phase regions in the T–P_{H_2} diagrams. For example, in the Mn-H system, the maximum hydrogen solubility in the α' and β primary solid solutions reaches $n \approx 0.06$–0.08, while the hydrogen content of the hydrides increases with the pressure from $n \approx 0.35$ to ≈ 0.5 for the γ-phase and from $n \approx 0.8$ to ≈ 0.95 for the ε-phase. In the Ni-H system, compositions of the γ_1 and γ_2 phases converge on going along the line of the $\gamma_1 \rightleftarrows \gamma_2$ equilibrium and get equal when the line terminates at a critical point.

The fact that phase equilibria in the Me-H systems vary systematically with increasing N^e and N^e_{eff} is most clearly seen for the series of the Fe-H, Co-H, and

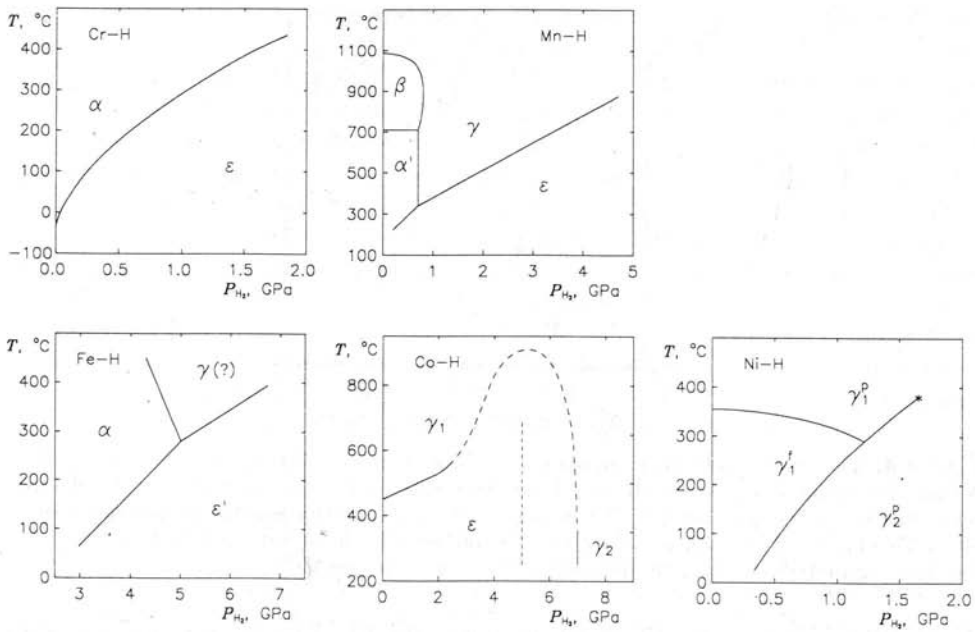

Figure 5. The T–P_{H_2} phase diagrams of the 3*d*-metals in the atmosphere of molecular hydrogen. Metal lattices of the phases: $\beta = \beta$-Mn type, other notations as in Fig. 1, γ_1 and γ_2 stand for the phases depleted and enriched in hydrogen, respectively. In the Co-H diagram, the dashed portion of the $\varepsilon \rightarrow \gamma$ boundary is tentative, and the vertical dashed line is a schematic plot of the line of supercritical anomalies of an isomorphous phase transformation in the virtual γ-solutions. In the Ni-H diagram, the line of the Curie points is shown for the ferromagnetic γ_1-phase, and the asterisk marks the position of the critical point of the $\gamma_1 \rightleftarrows \gamma_2$ transformation. The diagram for the Mn-H system is from ref. 1, for the Co-H system from ref. 16, and the other diagrams are from ref. 2.

Ni-H diagrams. The ε'-phase $FeH_{\approx 0.8}$ with $N^e_{eff} \lesssim 9$ el./metal atom has the same metal lattice as Co doped with Fe ($N^e < 9$ el./metal atom). The line of the $\varepsilon' \rightleftarrows \gamma$ transformation in the Fe-H system is smoothly substituted by the $\varepsilon \rightleftarrows \gamma$ line in the Co-H system with $N^e_{eff} \geq 9$ el./metal atom (in the Co-Fe alloys, the ε-phase is more stable than the ε'-phase at $N^e > 8.99$ el./metal atom). At higher pressures, the Co-H ε-solutions with $n \lesssim 0.6$ become less stable than the Co-H γ-solutions with the hydrogen concentration up to $n \approx 1$. That is, the metal lattice of the Co-H solutions changes for that of Ni ($N^e = 10$ el./metal atom) with increasing N^e_{eff}. The $\gamma_1 \rightleftarrows \gamma_2$ transformation, which is virtual in the Co-H system (it occurs between the metastable γ_1 and γ_2 phases in the region of thermodynamical stability of the ε-phase), becomes a transformation between the equilibrium phases in the Ni-H system. And finally, the Ni-H solutions with $n \lesssim 1.1$ and, correspondingly, with $N^e_{eff} \lesssim 11$ el./metal atom have the same *fcc* metal lattice as Cu ($N^e = 11$ el./metal atom).

In contrast to Fe, Co, and Ni, chromium and manganese do not form hydrides on the base of the same type of metal lattice as their successors in the Periodic Table, manganese and iron, respectively. The main cause is most likely that the pressure stabilizes the phases with minimum specific volume, whereas the modifications of manganese and iron, stable under ambient conditions, are not close-packed (note, that iron transforms to a close-packed ε modification in an inert medium at a pressure of 11–13 GPa at room temperature).

If only competition in the formation of different close-packed phases (γ, ε, ε', with the Sm-type metal lattice, *etc.*) is observed, one may expect the pressure effects

to be not so crucial, and analyze the role of the d-band filling. This seems to take place in the case of hydrogenation of $4d$-metals.

The most prominent evidence in support of the idea that the d-band occupancy mainly determines the crystal structure of the Group VI–VIII transition metals is that the metals of the $4d$ and $5d$ series exhibit the same $bcc \rightarrow hcp \rightarrow fcc$ sequence of crystal structures as the d-bands become progressively filled[13]. One can see from Fig. 1 that the dissolution of hydrogen in the $4d$-metals produces the same effect as an increase in N^e. The metal lattice of the hydride of bcc Mo ($N^e = 6$ el./atom) is hcp as that of Tc ($N^e = 7$ el./atom), the hydride of Tc has an hcp metal lattice as Ru ($N^e = 8$ el./atom), the hydride of Rh ($N^e = 9$ el./atom) is fcc as Pd ($N^e = 10$ el./atom), and the hydride of Pd is fcc as Ag ($N^e = 11$ el./atom).

What is more, the crystal structure sequence of the hydrides of $3d$-metals is the same as that of the hydrides of $4d$-metals except for the $dhcp$ lattice of the Fe hydride instead of the expected hcp one (Fig. 1).

As for the hydrides of alloys, most hydrides with $6.1 \leq N^e_{\text{eff}} \leq 7.1$ el./atom have closed packed metal lattices (hcp, fcc and their slightly distorted modifications) characteristic of most d-metals and alloys with N^e in the same range[2,4]. In the case of the RN type Nb_3Me alloys (Me = Os, Ir, Pt, and Au) with N^e ranging from 5.75 to ≈ 6.5 el./atom, the hydrides all have the same $A15$ metal structure as the starting alloys[5]. By analogy with what was said about the superconducting properties of these alloys in the previous chapter, the rigid d-band model predicts this structure at least for the cases with Me = Os, Ir, and Pt. One more and rather convincing observation is the CrB type metal lattice structure of the hydrides of the RN type ZrRu and HfRu alloys (A = Hf, Zr; B, C, ... = Ru, Rh, Pd, Pt, ...). This is the structure of the ZrPt and HfPt compounds[17] with $N^e = 7$ el./atom, which is close to $N^e_{\text{eff}} \approx$ 6.5–6.9 el./atom of the HfRu and ZrRu hydrides.

CONCLUSIONS

As is seen from the above, the rigid d-band model principally explains the available data on the crystal structure and physical properties of a rather large variety of transition metals and their alloys. This shows that the model takes into account one of the main effects of hydrogenation. Concluding, we would like to demonstrate how this model can be used to predict the effect of hydrogen on crystal structure and superconducting properties.

A good object for this purpose are the alloys with a σ-phase (type $D8_b$) structure, which form in many transition metal systems and have been rather thoroughly studied. In particular, niobium forms wide ranges of continuous solid σ-solutions with the $5d$-metals Re, Os, Ir, and Pt ($6 \lesssim N^e \lesssim 6.9$ el./atom). The T_c values of the alloys with $6 \lesssim N^e \lesssim 6.5$ el./atom are close to 2 K and nearly independent of N^e. At higher electron concentrations, they increase at an average rate of about 10 K per electron per atom, reach a maximum of about 5 K at $N^e \approx 6.7$ to 6.8 el./atom, and then begin to decrease[12].

The rigid d-band model predicts, correspondingly, that the hydrides with $N^e_{\text{eff}} \lesssim$ 6.9 el./atom will have metal lattices of the same $D8_b$ type. This is a bcc related structure, so the superconducting temperatures of the hydrides will follow Eq. (1). For example, the T_c value of the σ-type hydrides of the $Nb_{50}Re_{50}$ alloy ($N^e = 6$ el./atom) will decrease at the rate τ and vanish at $n \approx T_c(N^e)/\tau \approx 0.2$ to 0.4. The T_c value of the $Nb_{63}Ir_{37}$-H solid solutions ($N^e \approx 6.5$ el./atom) will remain approximately unchanged or will slowly decrease at $n \lesssim (6.8 - 6.5)/0.5 \approx 0.6$ until N^e_{eff} reaches the

position of the maximum of the $T_c(N^e)$ dependence, and begin to rapidly decrease at higher hydrogen concentrations.

REFERENCES

1. V.E. Antonov, T.E. Antonova, N.A. Chirin, E.G. Ponyatovsky, M. Baier, and F.E. Wagner, T–P phase diagram of the Mn-H system at pressures to 4.4 GPa and temperatures to 1000 °C, *Scripta Metal. Mater.*, to be published.
2. E.G. Ponyatovsky, V.E. Antonov, and I.T. Belash, High hydrogen pressures. Synthesis and properties of new hydrides, *in*: "Problems in Solid-State Physics," A.M. Prokhorov and A.S. Prokhorov, eds., Mir Publishers, Moscow, 1984, p. 109.
3. V.E. Antonov, I.T. Belash, V.F. Degtyareva, D.N. Mogilyansky, B.K. Ponomarev, and V.Sh. Shekhtman, Crystal structure and magnetic properties of high-pressure phases in the Fe-H and Fe-Cr-H systems, *Int. J. Hydrogen Energy* 14:371 (1989).
4. V.E. Antonov, T.E. Antonova, I.T. Belash, and V.I. Rashupkin, Superconductivities of high-pressure phases in the metal-hydrogen systems, *High Pressure Research* 1:315 (1989).
5. V.E. Antonov, T.E. Antonova, I.T. Belash, O.V. Zharikov, A.I. Latynin, A.V. Pal'nichenko, and V.I. Rashchupkin, Superconductivity of solid solutions of hydrogen in Nb_3Me compounds (Me = Au, Pt, Ir, Os) with the A15 structure, *Fiz. Tverd. Tela (Leningrad)* 31:12 (1989) [*Sov. Phys. Solid State* 31:1659 (1989)].
6. V.E. Antonov, E.L. Bokhenkov, A.I. Latynin, V.I. Rashupkin, B. Dorner, M. Baier, and F.E. Wagner, Crystal structure and superconductivity of high pressure hydrides and deuterides of HfRu and ZrRu compounds, *J. Alloys and Compounds* 209:291 (1994).
7. A.C. Switendick, Electronic band structures of metal hydrides, *Solid State Commun.* 8:1463 (1970); Electronic energy bands of metal hydrides — palladium and nickel hydride, *Ber. Bunsenges. Phys. Chem.* 76:535 (1972).
8. S.V. Vonsovsky. "Magnetizm," Izd. Nauka, Moscow (1971) [in Russian].
9. V.M. Pan, V.G. Prokhorov, and A.S. Shpigel. "Metal Physics of Superconductors," Izd. Naukova Dumka, Kiev (1984) [in Russian].
10. P.V. Gel'd, R.A. Ryabov, and L.P. Mokhracheva. "Hydrogen and Physical Properties of Metals and Alloys," Izd. Nauka, Moscow (1985) [in Russian].
11. A.I. Kolesnikov, I. Natcaniec, V.E. Antonov, I.T. Belash, V.K. Fedotov, J. Krawczyk, J. Mayer, and E.G. Ponyatovsky, Neutron spectroscopy of $MnH_{0.86}$, $NiH_{1.05}$, $PdH_{0.99}$ and harmonic behaviour of their optical phonons, *Physica B* 174:257 (1991).
12. S.V. Vonsovsky, Yu.A. Izyumov, and E.Z. Kurmaev. "Superconductivity of Transition Metals," Springer, Berlin, 1982.
13. H.L. Skriver, Crystal structure from one-electron theory, *Phys. Rev. B* 31:1909 (1985).
14. E. Wicke and H. Brodowsky, Hydrogen in palladium and palladium alloys, *in*: "Hydrogen in Metals II," G. Alefeld and J. Völkl, eds., *Topics in Appl. Phys.*, Vol. 29, Springer, Berlin (1978), p. 73.
15. B. Baranowski and K. Bocheńska, The free energy and entropy of formation of nickel hydride, *Z. Phys. Chem. N. F.* 45:140 (1965).
16. V.E. Antonov, T.E. Antonova, M. Baier, G. Grosse, and F.E. Wagner, On the isomorphous phase transformation in the solid fcc solutions Co-H at high pressures, *J. Alloys and Compounds*, to be published.
17. V.N. Kuznetsov, G.P. Zhmurko, and E.M. Sokolovskaya, Phase equilibria and structural stability of intermetallics in the Pt-Pd-Hf and Pt-Pd-Zr systems, *J. Less-Common Metals* 163:1 (1990).